Collective behavior of shear bands

V. F. Nesterenko[ac], M. A. Meyers[a] and T. W. Wright[b]

[a] Department of Applied Mechanics and Engineering Sciences
University of California, San Diego
La Jolla, CA 92093

[b] U. S. Army Research Laboratory
Aberdeen Proving Ground, Maryland 21005

[c] On leave from the Lavrentyev Institute of Hydrodynamics, Novosibirsk, Russia

The radial collapse of a thick-walled cylinder under high-strain-rate deformation ($\sim 10^4\ s^{-1}$) was used for the investigation of shear-band initiation and propagation in titanium and austentic stainless steel. The bands were observed to form on spiral trajectories and were periodically spaced. The frequency of initiation of the shear bands along the internal surface of the cylinder was established, and the spiral trajectory was compared with calculated values based on initiation of shear bands on surfaces of maximum shear strain. The shear-band spacing calculated from two existing theories was compared with the observed values. The theoretical predictions are found to give a reasonable first estimate for the actual spacings.

1. INTRODUCTION

Shear bands have been the object of research since the 19th century, when they were first observed and correctly interpreted by Tresca (for overviews, see 1994 special issue of Mech. of Matls. [1]). Numerous studies have adressed both mechanistic and microstructural features of shear bands. It is recognized that shear localization is a very important and often dominating damage mechanism for plastic deformation, especially at high strains and strain rates. A recurrent topic in studies of damage in materials is the question of spacing between damage sites. The ability to predict and possibly control significant features of the failure patterns, such as numbers, sizes, locations, and velocities of residual particles is dependent on a fundamental and quantitative understanding of evolution laws for these localized damage sites. A first step in obtaining an answer would be to estimate the spacing of initial nucleation sites since damage tends to grow in specific places in the material. Of course, this leaves out the questions of secondary damage, subsequent interaction of damage sites, and the like, but it is still a crucial beginning.

Whereas hundreds papers were devoted to the study of one isolated shear band, the analyses carried out by Grady and Kipp [2] and Ockendon and Wright [3] are the only theoretical efforts at elucidating their collective behavior. These analyses are based on momentum diffusion as unloading occurs within the band and pertubation analysis of rate dependent homogeneous shearing, respectively.

The objectives of this paper are to report observations of shear-band assemblages obtained under controlled initiation and propagation conditions and to compare these observations with these existing theories. An extended version of this report will be published elsewhere [2].

2. EXPERIMENTAL PROCEDURE AND RESULTS

The thick-walled cylinder technique was used; it was developed and is described by Nesterenko and coworkers [5, 6]. Figure 1(a) shows the experimental configuration used to produce the radial collapse of the metallic specimens. Two different metals were investigated: commercial purity titanium with equiaxed grains having average size of 72 μm and austentic stainless steel X18H9T (Soviet designation;analogous to 304L) with grain size of 30 μm. The system uses the controlled detonation of an explosive to generate the high pressures required for the collapse of a thick-walled cylinder. The metallic specimens are placed within a copper driver tube. The explosive is placed coaxially with the specimen and detonation is initiated at the top, propagating along the cylinder axis.

The state of stress generated within the collapsing cylinder is one of pure shear. This is shown in Figure 1(b), in which the distortion of an elemental cube at radius r_0 is followed as it moves towards the axis of the cylinder. The shear strain in the axial direction is zero, there is no rotation of the elemental cube and the material is assumed to be incompressible. The planes of maximum shearing lie at 45^0 to a radius and remain unrotated as deformation proceeds inwards, at least until shear bands develop. As the tube is collapsed inwards, its inner surface experiences increasing strains which tend to infinity as radius of the pore $R_f \rightarrow 0$. In the current investigation the initial radius of the internal cavity, R_0, was equal to 5.5 mm.

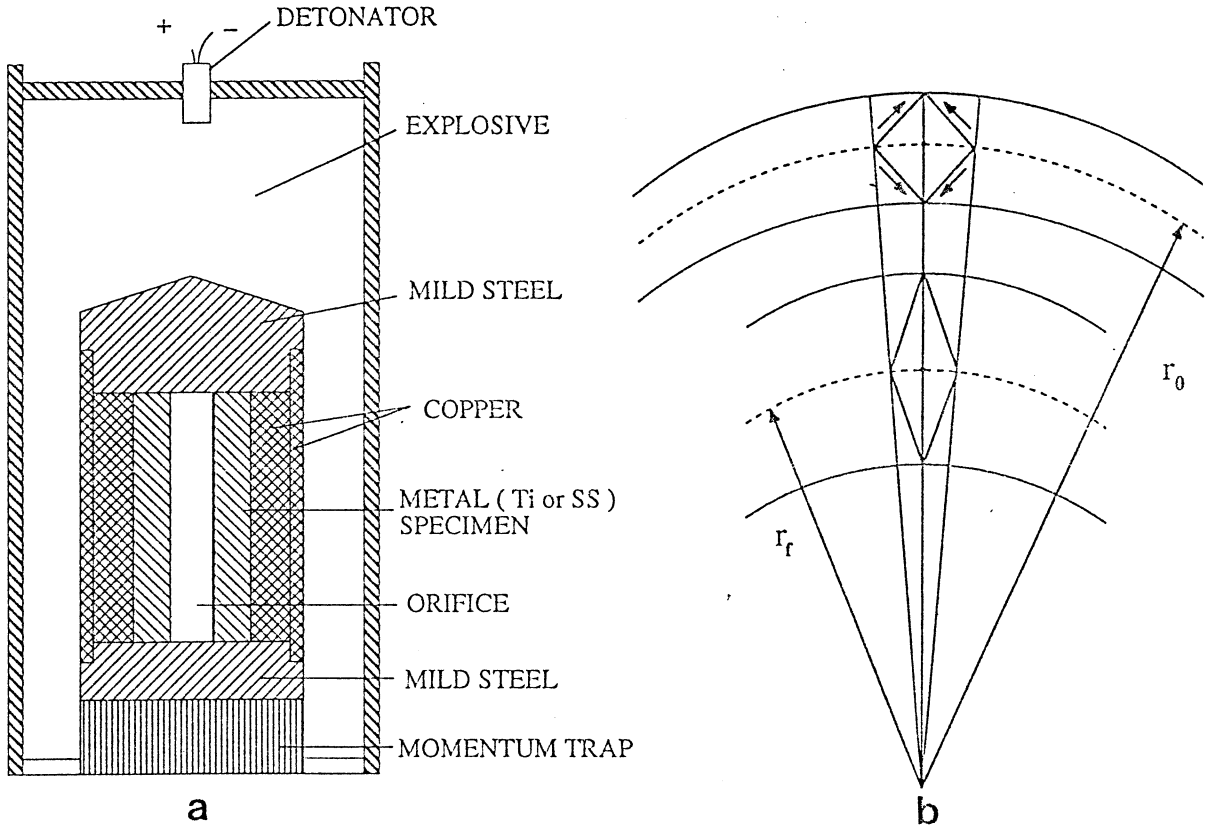

Figure 1. (a) Experimental configuration for collapse of thick-walled cylinder; (b) pure shear deformation of an element as tube collapses; (c) radial strains (as a function of normalized radius) during collapse for different initial radii; end points correspond to strains for complete collapse.

The radial, tangential, axial and maximum shear strains for this geometry are given by:

$$\varepsilon_{rr} = \ln\left(\frac{r_0}{r_f}\right) \qquad \varepsilon_{\varphi\varphi} = -\ln\left(\frac{r_0}{r_f}\right) = -\varepsilon_{rr} \qquad \varepsilon_{zz} = 0$$
$$\gamma = \left(2\, e^{2\varepsilon_{rr}} - 1\right)^{1/2} - 1 \tag{1}$$

The radii r_0 and r_f (Fig. 1b), representing the initial and final positions of a general point, are related by the conservation of mass, if deformation is uniform:

$$r_0^2 - R_0^2 = r_f^2 - R_f^2 \tag{2}$$

The strain rate for a general material point can be evaluated from the radial velocity of the cylindrical cavity v(t) , which was measured by an electromagnetic technique. The insertion of Ti or stainless steel cylinders inside a copper driver tube, shown in Figure 1(a), does not essentially change the time of collapse in comparison with the uniform copper cylinder having the same geometrical dimensions, because the overall mass (and initial velocity) does not change by more than 20 % (in case of Ti). This is why the velocity data obtained for a monolithic copper cylinder can be used, as a first approximation, to calculate the strain rate. For example, for a point on the inner cavity, the following relationship is used to calculate the shear strain rate at 45^0 to a radius:

$$\dot{\gamma} \approx 2\,\dot{\varepsilon}_{rr} = 2\,\frac{1}{R}\,\frac{dR}{dt} = 2\,\frac{v(t)}{\left(R_0 - \int_0^t v(t)dt\right)} \tag{3}$$

The strain rates in the specimens fluctuated around $3.5 \times 10^4\ s^{-1}$ (Ti) and $6 \times 10^4\ s^{-1}$ (SS).

Figure 2(a) shows the final appearance of the cross-section of the titanium specimen. The spiral shear bands forming around the cylinder axis are clearly seen. The traces of the shear bands show the pattern of growth in a clearer way; they are depicted in Figures 2(b) and 2(c) for titanium and stainless steel, respectively. The following observations can be made:

a) The shear bands initiate at the surface of the internal hole and propagate outwards;
b) The angle of the extremities of the shear bands with the radial directions fluctuates around 45^0, which is the plane of maximum shear stress (and strain). This is shown for three shear bands in Figure 2(b).
c) Most spirals have the same sense, clearly demonstrating that there exists a communication between the stress fields of the shear bands.
d) In the stainless steel specimen (see arrows in Fig. 2(c)) there are several bifurcation events. These are marked by arrows.

Two important simplifying assumptions are made in the analysis that follows:

a) The shear strains for shear band initiation and propagation are identical;
b) The shear bands form simultaneously.

With these assumptions, the radius r_f provides the critical shear strain γ_c for shear-band propagation. It is therefore possible to establish the value of the radius of the internal hole, R_i, at which initiation takes place.

The radius of the inner pore R_i , corresponding to the moment of shear initiation, can be found if the hypothesis is introduced that critical strains for shear-band initiation and propagation are equal. Using the Eqn. 1 for strains and the incompressibility condition(Eqn. 2) in case of complete collapse ($R_f = 0$):

$$R_i^2 = \frac{R_0^2\, r_f^2}{R_0^2 + r_f^2} \tag{4}$$

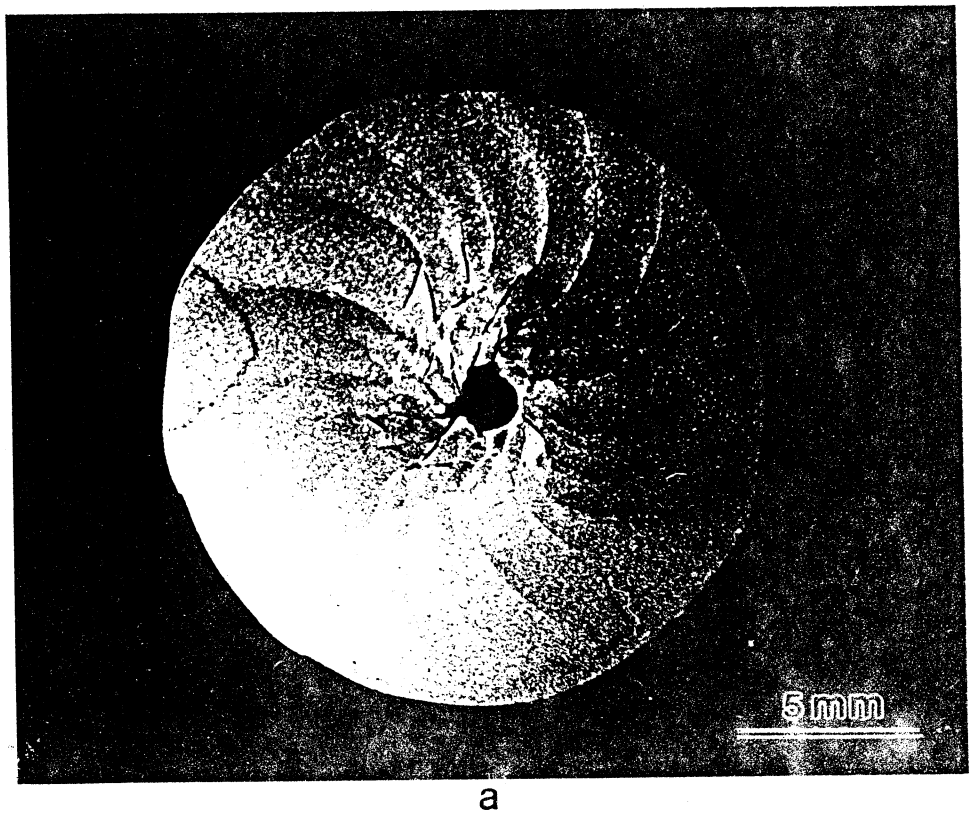

a

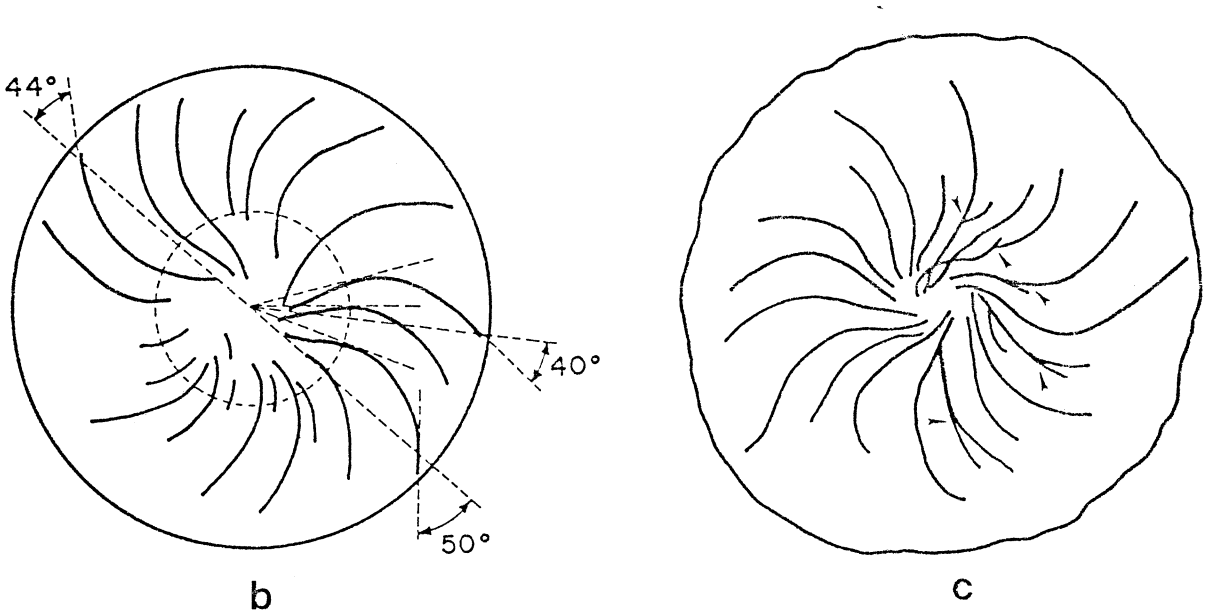

b c

Figure 2. Shear - band patterns on cross section of collapsed specimens; (a) optical micrograph for titanium; (b) tracing of shear bands for titanium; (c) tracing of shear bands for stainless steel.

Shear band spacings L, at a known R_i , can be obtained from the measured number of shear bands, N:

$$L = \frac{2\pi R_i}{N}\frac{1}{\sqrt{2}} \tag{5}$$

Analysis of shear-band traces of Figure 2 enables the calculation of the shear-band spacing at initiation, L_{exp}. The important parameters are given in Table 1. These values of L_{exp} are 1 and 0.85 mm at r_f for titanium and stainless steel, respectively. The critical shear strain for shear band propagation in titanium is found to be equal to 0.38; this is within the range of instability strains experimentally observed by Meyers et al [7] for the same material, using a hat-shaped specimen in a Hopkinson bar: 0.2 to 0.45. The corresponding temperature rise ΔT is on the order of 80 - 330 K. Localization at the shear band leads to much higher strains and temperatures, as calculated by Meyers et al. [7]. It is thought to be connected to dynamic recrystallization.

Table 1.
Experimental shear - band parameters for thick-walled cylinder method; shear band spacing L_{exp}, and number N.

Material	r_f, mm	R_i, mm	N	γ_c	$\dot{\gamma}$ (R_i), s^{-1}	Lexp, mm
Ti	8	4.5	20	0.22	3.5×10^4	1
SS	5.5	3.9	21	0.4	6×10^4	0.85

3. ANALYTICAL PREDICTIONS

It is possible to compare the observed spacing between shear bands with predictions from calculations by Grady and Kipp(GK) [2] for rate independent materials or the more recent result given by Ockendon and Wright(OW) [3] for rate dependent materials.

The basic notion, used in the GK analysis, is that rapid loss of strength or ability to transfer shearing tractions across the developing shear band affects neighboring material by forcing it to unload. The predicted spacing is given as

$$L_{GK} = 2\left\{9\,k\,C/\dot{\gamma}_0^3\,a^2\,\tau_0\right\}^{1/4} \tag{6}$$

In this equation the applied shear strain rate is $\dot{\gamma}_0$, and the relation between flow stress and temperature is assumed to be

$$\tau = \tau_0\,(1 - a\,\vartheta) \tag{7}$$

where τ_0 is the strength at a reference temperature T_0, ϑ is the relative temperature $T\text{-}T_o$, a a softening term, and C is the heat capacity.

The OW analysis is based on the notion that shear bands arise from small, but growing disturbances in an otherwise uniform region of constant strain rate. Disturbances do not propagate in perpendicular directions, but simply grow in place, so the most likely minimum spacing is obtained by finding the fastest growing wavelength. The resulting spacing, L_{OW}, (to lowest order terms) is:

$$L_{OW} = 2\pi\left\{\frac{m^3\,k\,C}{\dot{\gamma}_0^3\,a^2\,\tau_{h0}}\right\}^{1/4} \tag{8}$$

Although the approaches taken by GK and OW are completely different, it is a remarkable fact that except for numerical factors and the rate constants, the two results are the same.

The GK and OW formulations were applied to the materials tested in Section 2 by means of the use of Equations 6 and 8 , respectively. They enabled the calculation of the shear-bands spacings L_{GK} and L_{OW} respectively. Data for Ti were taken from Meyers et al. [2] and data for SS from Folansbee [8] and Epshtein [9].

The physical parameters in the GK and OW models and the calculated shear-bands spacings L_{GK} and L_{OW} are presented in Table 2. It is seen that both models provide reasonable estimates of L, and are in agreement with the experimental results (Table 1). Taking into account the one - dimensional character of the models and three - dimensional geometry of experiments, the agreement of both theoretical predictions with experimental results should be considered satisfactory.

It should be mentioned that the OW model describes only the spacings between initiation sites for shear bands, whereas the GK model describes the spacing of fully formed bands. If the spacing of shear bands is determined by their initiation, the OW model should be obeyed. On the other hand, if propagation establishes the spacing, the GK model should dominate. It seems clear that the OW analysis successfully predicts the initiation for Ti and SS. The bifurcation of the shear bands (Figure 2(c)) is possibly indicative of a momentum - diffusion(GK) process: once the bands reach a spacing above a critical value, new bands are formed to accomplish the deformation.

Table 2.
Material parameters and theoretical predictions of shear-band spacing, L, for Ti and SS.

Material	m	τ_0 (τ_{h0}), MPa	k, J /s m K	C, J / kg K	a x10^4, K^{-1}	L_{GK}, mm	L_{OW}, mm
Ti	0.033	1300	19	528	15	1.8	0.3
SS	0.05	1100	14.7	460	7.2	1.7	0.3

4. COMPARISON OF PREDICTED AND OBSERVED SHEAR - BAND MORPHOLOGY

The shear band morphology can be obtained by calculating the trajectory of the tip of the shear localization region. The following assumptions were made:

1. The overall movement of the material, at distances relatively far outside the central hole, is radially convergent with an axis of symmetry coincident with the axis of the cylinder. In actual deformation, the geometrical constraints are such that an additional bending of the shear segments is required for the total collapse of the void.
2. The critical effective strains for shear band initiation and propagation are identical and independent of strain rate. Under pure shear, the hypothesis of critical effective strain or critical shear strain are identical.
3. Shear-band initiation takes place at the internal surface of the hole and all shear bands are created simultaneously.
4. The tip of a shear band propagates along the surfaces of maximum shear strain.
5. Material is incompressible.

It was possible to develop an equation that describes the shear-band trajectories. The derivation is given in [4] and will not be reproduced here. Only the final equation and its graphical representation are given. The entire assemblage of shear bands can be represented by assuming that they create a periodical array with spacing L and the same sense. In order to do this in a more general way, the critical shear strain for shear band initiation is used to replace r_f ; thus, the solution acquires generality. The number of shear bands forming on the

circumference has to be an integer, and therefore the calculated number i has to have an integral upper bound, which is indicated by *"int"* below. Each solution i represents one curve.

$$\theta_i = e^{\gamma_c/2}\left\{\frac{i\sqrt{2}L}{R_0} + \frac{e^{\gamma_c/2}}{2}\ln\left(1+\frac{r^2}{R_0^2}\right)\right\}$$
$$int\left(\frac{2\pi R_0}{\sqrt{2}L}e^{-\frac{\gamma_c}{2}}\right) \geq i \geq 1 \qquad (9)$$

Equation 9 represents the entire assemblage of the shear bands; L can be the experimental (L_{exp}) or calculated (L_{OW}, L_{GK}) spacing. Figure 3 shows the application of Equation 9 to the constitutive behavior of titanium. The correspondence of the shape of the curves with the actual experimental results (Figure 3(b)) is satisfactory. It should be noted that the regions within the dashed circle of Figure 6 show considerable deviation from the experimental configuration (Fig. 3b)because additional bending of the shear zones is kinematically necessary for total collapse; this effect is not incorporated into analysis.

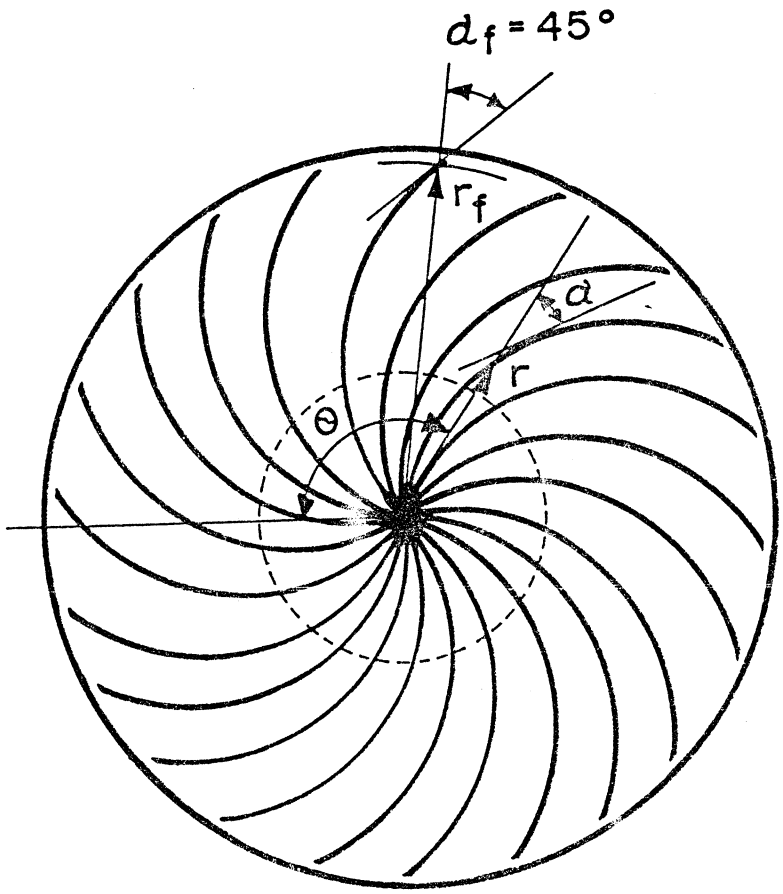

Figure 3. Calculated shear - band pattern produced by collapse of thick - walled cylinder; number of shear bands N = 20 and radius r_f = 8 mm for shear band extremity correspond to experimental values for Ti.

5. SUMMARY AND CONCLUSIONS

It has been experimentally demonstrated, using the high-strain radial collapse of thick-walled cylinders of titanium and stainless steel, that shear bands undergo a self-organization process as they initiate and propagate. Mainly one direction of spiral shear bands - either clockwise or counterclockwise - was observed in each experimental event. The spiral trajectories correspond to surfaces of maximum shear strain. The array of shear bands, diverging from the initiation region, on the internal surface of the thick-walled cylinder, is periodic, with a characteristic spacing. For stainless steel, bifurcation of the shear bands is observed to occur at a critical strain (or radius).

The experimental results are compared with predictions of two theories, and the experimentally obtained shear band spacings (0.9 mm (SS) and 1 mm (Ti)) are in good agreement with the predictions of Grady-Kipp(1.7 mm (SS) and 1.8 mm (Ti)) and Ockendon-Wright(0.3 mm (SS and Ti)). It is felt that the OW theory predicts better the shear band spacing if it is mainly determined by the initiation stage, whereas the propagation is affected by the momentum diffusion in the GK approach. Prior to the onset of localization, momentum diffusion is absent, and its role is only fully felt in the propagation stage. The trajectories of the shear bands are modeled, enabling a prediction of the final configuration in good agreement with observations.

Acknowledgements: This research is supported by the U. S. Army Research Office, Contract DAAH 04-94-G-031, by the U. S. Office of Naval Research, Contract N00014-94-1-1040 and by the U.S.Army Research Laboratory. Authors wish to acknowledge the valuable help in conducting experiments by Dr. M.P. Bondar and Ya.L. Lukyanov(Lavrentyev Institute of Hydrodynamics, Novosibirsk, Russia), as well as Mr. H.C. Chen and Prof. K.S. Vecchio (UCSD) for help in metallography.

REFERENCES

1. Mechanics of Materials (Special Issue on Shear Instabilities and Viscoplasticity Theories) 17, (1994).
2. D.E. Grady and M.E. Kipp, J. Mech. Phys. Solids, 35 (1987) 95.
3. H. Ockendon and T.W. Wright, Int. J. Plasticity (to be published).
4. V.F. Nesterenko, M.A. Meyers, and T. W. Wright, "Self-Organization of Shear Bands in High-Strain-Rate Deformation", Acta Met. Mat., submitted (1995).
5. V.F. Nesterenko and M.P. Bondar, DYMAT Journal, 1 (1994) 245.
6. V.F. Nesterenko, M.A. Meyers, H.C. Chen, and J.C. LaSalvia, Applied Physics Letters, 65 (1994) 3069.
7. M.A. Meyers, G. Subhash, B.K. Kad, and L. Prasad, Mechanics of Materials, 17 (1994) 175.
8. P.S. Follansbee, in Metallurgical Aplications of Shock-Wave and High-Strain-Rate Phenomena, Eds. L.E. Murr, K.P. Staudhammer, and M.A. Meyers, Marcel Dekker, New York and Basel, (1986), p. 451.
9. G.N. Epshtein, The Structure of Explosively Deformed Metals, Moscow, Metallurgy, 1988(in Russian), p. 66.